Commun Nonlinear Sci Numer Simulat 14 (2009) 2178–2189

Contents lists available at ScienceDirect

Commun Nonlinear Sci Numer Simulat

journal homepage: www.elsevier.com/locate/cnsns

MHD power-law fluid flow and heat transfer over a non-isothermal stretching sheet

K.V. Prasad [a,*], Dulal Pal [b], P.S. Datti [c]

[a] Department of Mathematics, Central College Campus, Bangalore University, Bangalore 560 001, India
[b] Department of Mathematics, Siksha Bhavana, Visva-Bharati University, Santiniketan, West Bengal 731 235, India
[c] TIFR Centre, IISc-TIFR Joint Programme in Applications of Mathematics, Indian Institute of Science (IISc), Bangalore 560 012, India

ARTICLE INFO

Article history:
Received 25 April 2008
Received in revised form 20 June 2008
Accepted 20 June 2008
Available online 5 July 2008

PACS:
44.20.+b
47.11.Bc
47.15.Cb
47.50.Cd
02.60.Lj

Keywords:
Stretching sheet
Power-law fluid
Thermal conductivity
Boundary layer
Heat transfer
Magnetohydrodynamics

ABSTRACT

This article presents a numerical solution for the magnetohydrodynamic (MHD) non-Newtonian power-law fluid flow over a semi-infinite non-isothermal stretching sheet with internal heat generation/absorption. The flow is caused by linear stretching of a sheet from an impermeable wall. Thermal conductivity is assumed to vary linearly with temperature. The governing partial differential equations of momentum and energy are converted into ordinary differential equations by using a classical similarity transformation along with appropriate boundary conditions. The intricate coupled non-linear boundary value problem has been solved by Keller box method. It is important to note that the momentum and thermal boundary layer thickness decrease with increase in the power-law index in presence/absence of variable thermal conductivity.

1. Introduction

The study of two-dimensional boundary layer flow over a stretching sheet has gained much interest in recent times because of its numerous industrial applications viz in the polymer processing of a chemical engineering plant and in metallurgy for the metal processing. Crane [1] was first to formulate this problem to study a steady two-dimensional boundary layer flow caused by stretching of a sheet that moves in its plane with a velocity which varies linearly with the distance from a fixed point on the sheet. Many investigators have extended the work of Crane [1] to study heat and mass transfer under different physical situations (e.g., Gupta and Gupta [2], Chen and Char [3], Datta et al. [4], McLeod and Rajagopal [5], Chaim [6,7]) by including quadratic and higher order stretching velocity. All these works are restricted to Newtonian fluid flows which have received much attention in the last three decades due to their occurrence in nature and their increasing importance in industry. Different types of non-Newtonian fluids are visco-elastic fluid, couple stress fluid, micro polar fluid and power-law fluid. Rajagopal et al. [8] and Siddappa and Abel [9] studied the flow of a visco-elastic fluid flow over a stretching sheet. Troy et al. [10], Wen-Dong [11], Sam Lawrence and Rao [12], McLeod and Rajagopal [5] have discussed the problem of uniqueness/non-uniqueness of the flow of a non-Newtonian visco-elastic fluid over a stretching sheet. Abel and Veena [13]

* Corresponding author. Tel.: +91 80 22961433.
E-mail address: kvprasad@yahoo.co.in (K.V. Prasad).

1007-5704/$ - see front matter © 2008 Elsevier B.V. All rights reserved.
doi:10.1016/j.cnsns.2008.06.021

Nomenclature

A, D	constants
b	stretching rate, positive constant
C_f	skin friction
C_p	specific heat at constant pressure
f	dimensionless velocity variable
$h(x)$	heat transfer coefficient
H_0	applied transverse magnetic field
$k(T)$	thermal conductivity
k_∞	thermal conductivity far away from the sheet
l	characteristic length
n	power-law index
Nu_x	Nusselt number
Pr_n	generalized modified Prandtl number for power-law fluids
Q_s	internal heat generation/absorption
q_w	local heat flux at the sheet
Re_x	local Reynolds number
T	temperature variable
T_w	given temperature at the sheet
T_∞	constant temperature of the fluid far away from the sheet
x	horizontal distance
y	vertical distance
u	velocity in x-direction
U	velocity of the sheet
v	velocity in y-direction

Greek symbols

α	constant >0
β	heat source/sink parameter
ΔT	sheet temperature
ε	small parameter
η	similarity variable
γ	kinematic viscosity
μ_m	magnetic permeability
ψ	stream function
ρ	density
σ	electrical conductivity
τ_{xy},τ_{ij}	shear stress
θ	dimensionless temperature variable

studied the heat transfer of a visco-elastic fluid over a stretching sheet. Bujurke et al. [14] have investigated the heat transfer phenomena in a second order fluid flow over a stretching sheet with internal heat generation and viscous dissipation. Prasad et al. [15] analyzed the problem of a visco-elastic fluid flow and heat transfer in a porous medium over a non-isothermal stretching sheet with variable thermal conductivity. Prasad et al. [16] have investigated on the diffusion of a chemically reactive species of a non-Newtonian fluid immersed in a porous medium over a stretching sheet.

All the above-mentioned research work do not however consider the situations where hydromagnetic effects arise. The study of hydrodynamic flow and heat transfer over a stretching sheet may find its applications in polymer technology related to the stretching of plastic sheets. Also, many metallurgical processes involve the cooling of continuous strips or filaments by drawing them through a quiescent fluid and while drawing these strips are sometimes stretched. The rate of cooling can be controlled by drawing such strips in an electrically conducting fluid subjected to a magnetic field in order to get the final products of desired characteristics as the final product greatly depend on the rate of cooling. In view of this, the study of MHD flow of Newtonian/non-Newtonian flow over a stretching sheet was carried out by many researchers (Sarpakaya [17], Pavlov [18], Chakrabarti and Gupta [19], Char [20], Andersson [21], Datti et al. [22]). These works however do not consider the study of a non-Newtonian power-law fluid model. The simplest and most common type of such a model is the Ostwald-de Waele model i.e. power-law fluid for which the rheological equation of the state between the stress components τ_{ij} and strain components e_{ij} is defined by Vujannovic et al. [23]

$$\tau_{ij} = -p\delta_{ij} + K\left|\sum_{m=1}^{3}\sum_{l=1}^{3} e_{lm}e_{lm}\right|^{\frac{n-1}{2}} e_{ij}, \tag{1.1}$$

where p is the pressure, δ_{ij} is Kroneckar delta and K and n are, respectively, the consistency coefficient and power-law index of the fluid. Such fluids are known as power-law fluid. For $n > 1$, fluid is said to be dilatant or shear thickening; for $n < 1$, the fluid is called shear thinning or pseudo-plastic fluid and for $n = 1$, the fluid is simply the Newtonian fluid. Several fluids studied in the literature suggest the range $0 < n \leqslant 2$ for the value of power-law index n.

Keeping this in view, in the present paper, we study the effect of variable thermal conductivity on the heat transfer of a non-Newtonian power-law fluid, subjected to a magnetic field, over a non-isothermal stretching sheet with internal heat generation/absorption. This is in contrast to the work of Andersson et al. [24] and Jadhav and Waghmode [25], where constant thermal conductivity was considered. It has been observed by Savvas et al. [26] that for liquid metals, the thermal conductivity varies linearly with temperature in the range 0–400 °F. Hence, we have assumed that the thermal conductivity is a linear function of the temperature. Further, we consider two cases of non-isothermal boundary conditions namely,

(1) Surface with prescribed surface temperature (PST Case) and
(2) Surface with prescribed wall heat flux (PHF Case).

Because of the rheological equation of state Eq. (1.1), the momentum and energy equations are highly non-linear, and coupled form of partial differential equations (PDEs). These PDEs are then converted to coupled non-linear ordinary differential equations (ODEs) by using the similarity variables along with the appropriate boundary conditions. In this paper, we propose to solve these ordinary differential equations numerically by Keller box method [27,28]. One of the important findings is that the horizontal boundary layer thickness decreases with the increase of power-law index. The thickness is much larger for shear thinning (pseudo plastic) fluids ($n < 1$) than that of Newtonian ($n = 1$) and shear thickening (dilatants) fluids ($n > 1$).

2. Governing equations and similarity analysis

We consider two-dimensional steady, laminar flow of an incompressible and electrically conducting fluid obeying power-law model in the presence of a uniform transverse magnetic field over a non-isothermal stretching sheet. The flow is generated due to the stretching of the sheet by applying two equal and opposite forces along the x-axis by keeping the origin fixed and considering the flow to be confined to the region $y > 0$. In order to obtain the temperature difference between the surface and the ambient fluid, we consider the temperature dependent heat source/sink in the flow. In this situation, the basic governing equations of continuity and momentum (Andersson et al. [21], Chiam [29]) take the following form

$$\frac{\partial u}{\partial x}+\frac{\partial v}{\partial y}=0, \tag{2.1}$$

$$u\frac{\partial u}{\partial x}+v\frac{\partial u}{\partial y}=-\nu\frac{\partial}{\partial y}\left(-\frac{\partial u}{\partial y}\right)^{n}-\frac{\sigma\mu_{\mathrm{m}}^{2}H_{0}^{2}}{\rho}u, \tag{2.2}$$

where u and v are the flow velocity components in the stream-wise (x) and cross-stream (y) directions, respectively. ν is the kinematic viscosity of the fluid, σ is the electrical conductivity, μ_{m} is the magnetic permeability, H_0 is the applied transverse magnetic field and ρ is the fluid density. The first term in the right hand side of the Eq. (2.2) i.e. the shear rate ($\partial u/\partial y$) has been assumed to be negative throughout the entire boundary layer since the stream-wise velocity component u decreases monotonically with the distance y from the moving surface. A rigorous derivation and subsequent analysis of the boundary layer equations for power-law fluids were recently provided by Denier and Dabrowski [30]. They focused on boundary layer flow driven by free stream $U(x)\approx x^{m}$ which is of the Falkner-Skan type. Such boundary layer flows are driven by a stream wise pressure gradient $-\frac{\mathrm{d}p}{\mathrm{d}x}=\rho\frac{\mathrm{d}u}{\mathrm{d}x}$ set up by the external free stream outside the viscous boundary layer. In the present context no driving pressure gradient is present. Instead the flow is driven solely by a flat surface which moves with a prescribed velocity $U(x) = bx$, where x denotes the distance from the slit from which the surface emerges and $b > 0$. Thus, the relevant boundary conditions applicable to the flow are

$$u(x,0)=U(x), \tag{2.3a}$$

$$v(x,0)=0, \tag{2.3b}$$

$$u(x,y)\to 0 \quad \text{as } y\to\infty. \tag{2.3c}$$

Here, Eq. (2.3c) claims that the stream-wise velocity vanishes outside the boundary layer, the requirement Eq. (2.3b) signifies the importance of impermeability of the stretching surface whereas Eq. (2.3a) assures no slip at the surface. Following transformation is introduced in accordance with Andersson and Dandapat [31]:

$$\eta=\frac{y}{x}(Re_x)^{\frac{1}{n+1}},\quad \psi(x,y)=Ux(Re_x)^{\frac{-1}{n+1}}f(\eta), \tag{2.4}$$

where η is the similarity variable and $\psi(x,y)$ is the stream function. The velocity components u and v are given by

$$u=\frac{\partial\psi}{\partial y},\quad v=-\frac{\partial\psi}{\partial x}. \tag{2.5}$$

The local Reynolds number is defined by

$$Re_x = \frac{U^{2-n}x^n}{\nu}. \tag{2.6}$$

The mass conservation Eq. (2.1) is automatically satisfied by Eq. (2.5). By assuming the similarity function $f(\eta)$ to depend on the similarity variable η, the momentum Eq. (2.2) is transformed into ordinary differential equation

$$n|-f''|^{n-1}f''' - f'^2 + \left(\frac{2n}{n+1}\right)ff'' - M_n f' = 0, \tag{2.7}$$

where $M_n = \frac{\sigma\mu_m^2 H_0^2}{\rho b}$ is the magnetic parameter. Eq. (2.7) is solved numerically subject to the following boundary conditions obtained from Eq. (2.3) using Eq. (2.4) as

$$f(\eta) = 0 \quad \text{at} \quad \eta = 0, \tag{2.8a}$$
$$f'(\eta) = 1 \quad \text{at} \quad \eta = 0, \tag{2.8b}$$
$$f'(\eta) \to 0 \quad \text{as} \quad \eta \to \infty. \tag{2.8c}$$

It should be noted that the velocity $U = U(x)$ is used to define the dimensionless stream function ψ in the Eq. (2.4) and the local Reynolds number in Eq. (2.6) describes the velocity of the moving surface that drives the flow. This choice coincides with the conventional boundary layer analysis, in which the free stream velocity is taken as the velocity scale. The transformations defined in Eq. (2.4) and Eq. (2.5) can be used for arbitrary variation of $U(x)$, so the transformation results in a true similarity problem only if U varies as bx. Therefore, such surface velocity variations are required for the ordinary differential Eq. (2.7) to be valid. Non-Similar stretching sheet problems which require the solution of partial differential equations rather than ordinary differential equations were considered by several researchers for Newtonian fluids. Three boundary conditions (2.8a–c) are sufficient for solving the third-order equation which results for transformed momentum equations for power-law fluids.

The equation for a Newtonian fluid can be obtained as a special case if one puts $n = 1$ in Eq. (2.7). In this case we have,

$$f''' - f'^2 + ff'' - M_n f' = 0, \tag{2.9}$$

with boundary conditions (2.8a–c).

It is interesting to note that the Eq. (2.9) has exact analytical solution of the form

$$f' = e^{-\alpha\eta}, \quad \alpha > 0, \tag{2.10}$$

satisfying the boundary conditions (2.8 a–c).

Integration of Eq. (2.10) and using (2.8a) gives

$$f = \frac{1}{\alpha}(1 - e^{-\alpha\eta}), \quad \text{where } \alpha = \sqrt{(1 + M_n)}. \tag{2.11}$$

The skin friction coefficient C_f at the sheet is given by

$$C_f = -\left(\frac{2\tau_{xy}}{\rho(bx)^2}\right)_{y=0} = 2[-f''(0)]^n [Re_x]^{\frac{-1}{n+1}}, \tag{2.12}$$

where τ_{xy} is the shear stress and Re_x is the local Reynolds number. We now discuss the heat transport in the above flow due to a stretching sheet.

3. Heat transfer

The energy equation for a fluid with variable thermal conductivity in the presence of internal heat generation/absorption for the two-dimensional flow is given by (Chiam [29]):

$$\rho c_p u\frac{\partial T}{\partial x} + \left(\rho c_p v - \frac{\partial \kappa(T)}{\partial y}\right)\frac{\partial T}{\partial y} = \kappa(T)\frac{\partial^2 T}{\partial y^2} + Q_s(T - T_\infty), \tag{3.1}$$

where c_p is the specific heat at constant pressure, T is the temperature of the fluid, T_∞ is the constant temperature of the fluid far away from the sheet and $\kappa(T)$ is the temperature-dependent thermal conductivity. We consider the temperature-thermal conductivity relationship of the following form (Chiam [29]):

$$\kappa(T) = \kappa_\infty\left(1 + \frac{\varepsilon}{\Delta T}(T - T_\infty)\right), \tag{3.2}$$

where $\Delta T = T_w - T_\infty$, T_w is the sheet temperature, ε is a small parameter and κ_∞ is the conductivity of the fluid far away from the sheet. The term containing Q_s in Eq. (3.1) represents the temperature-dependent volumetric rate of heat source when $Q_s > 0$ and heat sink when $Q_s < 0$. These deal with the situation of exothermic and endothermic chemical reactions, respectively.

Substituting Eq. (3.2) in Eq. (3.1), we get

$$\rho c_p u\frac{\partial T}{\partial x}+\left(\rho c_p v-\frac{k_\infty \varepsilon}{\Delta T}\frac{\partial T}{\partial y}\right)\frac{\partial T}{\partial y}=\kappa_\infty\left(1+\frac{\varepsilon}{\Delta T}(T-T_\infty)\right)\frac{\partial^2 T}{\partial y^2}+Q_s(T-T_\infty). \tag{3.3}$$

The thermal boundary conditions depend on the type of heating process under consideration. Here, we consider two different heating processes, namely, (i) prescribed surface temperature and (ii) prescribed wall heat flux, varying with the distance. The boundary conditions assumed for solving Eq. (3.3) are

$$\left.\begin{array}{ll} T=T_w\left[=T_\infty+A\left(\frac{x}{l}\right)\right] & \text{(PST Case)}\\ -k\frac{\partial T}{\partial y}=q_w=D\left(\frac{x}{l}\right) & \text{(PHF Case)}\end{array}\right\}\quad \text{at } y=0 \text{ and} \tag{3.4}$$

$$T\to T_\infty \quad \text{as } y\to\infty, \tag{3.5}$$

where A is a constant. It is obvious now that

$$\Delta T=T_w-T_\infty=\begin{cases} A\left(\frac{x}{l}\right) & \text{PST Case}\\ \frac{D}{k_\infty}\left(\frac{x}{l}\right)(Re_x)^{\frac{-1}{n+1}}x & \text{PHF Case}\end{cases}. \tag{3.6}$$

We now use a scaled η-dependent temperature of the form

$$\theta(\eta)=\frac{T-T_\infty}{\Delta T}. \tag{3.7}$$

The imminent advantage of using Eq. (3.4) is that the temperature-dependent thermal conductivity turns out to be x-independent. Eq. (3.3) reduces to the non-linear differential equation using Eq. (2.4):

$$(1+\varepsilon\theta)\theta''+\varepsilon\theta'^2+Pr\left(\frac{2n}{n+1}(f\theta'-(f'-\beta)\theta)\right)=0, \tag{3.8}$$

where, $Pr=\left(\frac{\gamma^2 b^{3(n-1)}x^{2(n-1)}}{\alpha^{n+1}}\right)^{\frac{1}{n+1}}$ is the generalized Prandtl number for power-law fluid and $\beta=\frac{Q_s}{\rho c_p b}$, is the heat source/sink parameter.

Eq. (3.4) on using Eqs. (3.5) and (3.6) can be written as

$$\left.\begin{array}{ll}\theta(0)=1 & \text{(PST Case)}\\ \theta'(0)=-1 & \text{(PHF Case)}\end{array}\right\},\quad \theta(\infty)=0. \tag{3.9}$$

The local Nusselt number is given by

$$Nu_x=\frac{h(x)}{K_\infty}, \tag{3.10}$$

where the heat transfer coefficient $h(x)$ is of the form

$$h(x)=\frac{q_w(x)}{\Delta T} \tag{3.11}$$

and the local heat flux at the sheet is

$$q_w=-K_\infty\left(\frac{\partial T}{\partial y}\right)_{\text{at } y=0}=-K_\infty Ax(Re_x)^{1/(n+1)}\theta'(0). \tag{3.12}$$

Substituting Eqs. (3.4), (3.11) and (3.12) in Eq. (3.10), we get

$$Nu_x=-Re_x^{\frac{1}{n+1}}\theta'(0). \tag{3.13}$$

4. Numerical procedure

Since the equation for f does not involve $\theta(\eta)$, so we use Keller Box method (Cebeci and Bradshaw [27], Keller [28] and Press et al. [32]) to compute f numerically. The resulting system of algebraic equations has been solved by a tridiagonal block solver [27]. The choice of numerical value of η_∞, which obviously depends on the physical parameters n and M_n, is very crucial in this numerical procedure. The initial guess was made from the known exact solution for $n = 1$, and several trial and error runs were made to obtain accurate values of f, f_η etc. up to a significant number of decimal places that satisfy the boundary condition at η_∞. Similarly, to obtain $\theta(\eta)$ numerically, we use the values of f obtained from Keller box method and employ a shooting technique (Conte and de Boor [33]). Here also, the initial guess was made with the help of the known exact solution for $\varepsilon = 0$, $Pr = 1$ and $n = 1$. The numerically computed values are then used for plotting several graphs and tabulate results in Tables.

5. Results and discussion

The numerical computation is carried out for different values of magnetic parameter Mn, power-law index n, Prandtl number Pr, variable thermal conductivity parameter ε and heat source/sink parameter β using the numerical procedure discussed in the previous section. In order to get a clear insight of the physical problem, the horizontal velocity profiles $f_\eta(\eta)$ and temperature profiles $\theta(\eta)$ for both PST and PHF cases have been discussed by assigning the numerical values to the non-dimensional parameters encountered in the problem. The numerical results are shown graphically in Figs. 1–6. To assess the accuracy of the numerical method used, the computed value of the skin friction co-efficient and rate of heat transfer were compared with those obtained by Andersson [21] for different values of physical parameters. It is observed that our results are in good agreement with the results obtained by the previous investigators as seen from the tabulated results in Table 1.

Figs. 1 and 2 illustrate the effect of power-law index n and magnetic parameter Mn on the horizontal velocity profiles $f_\eta(\eta)$ with η. It is noticed from these figures that the horizontal velocity profiles decrease with increasing the values of power-law index n and magnetic parameter Mn in the boundary layer but this effect is not very prominent near the wall. The effect of increasing the value of the power-law index parameter n is to reduce the horizontal velocity and thereby reducing boundary layer thickness i.e. the thickness is much large for shear thinning (pseudo plastic) fluids ($0 < n < 1$) than that of Newtonian ($n = 1$) and shear thickening (dilatant) fluids ($1 < n < 2$), as clearly seen from Fig. 1. The effect of magnetic parameter Mn on the horizontal velocity profile is depicted in Fig. 2. It is observed that the horizontal velocity profile decreases with increase in the magnetic field parameters due to the fact that, the introduction of transverse magnetic field (normal to the flow direction) has a tendency to create a drag, known as Lorentz force which tends to resist the flow. This behavior is even true in the case of shear thickening and shear thinning fluids.

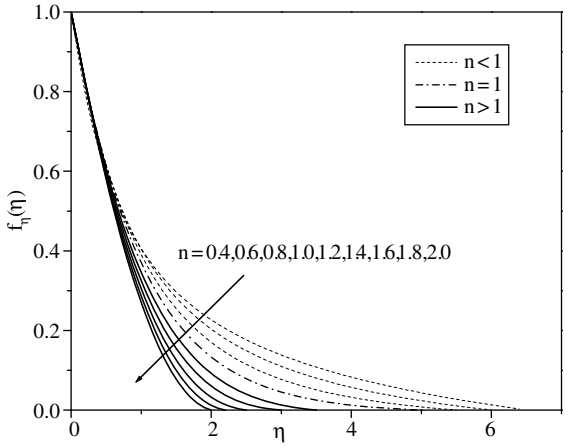

Fig. 1. Horizontal velocity profiles $f_\eta(\eta)$ vs. η for different values of n with $Mn = 0$.

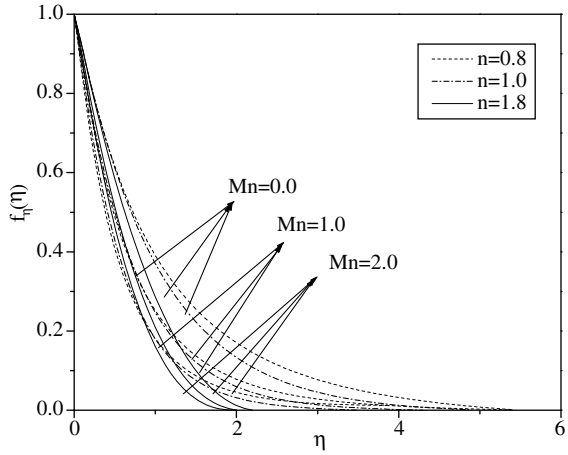

Fig. 2. Horizontal velocity profiles $f_\eta(\eta)$ vs. η for different values of Mn and n.

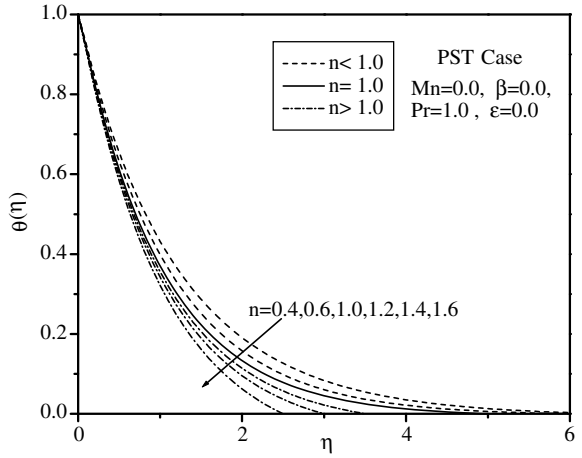

Fig. 3a. Variation of temperature profiles $\theta(\eta)$ vs. η for different values of n.

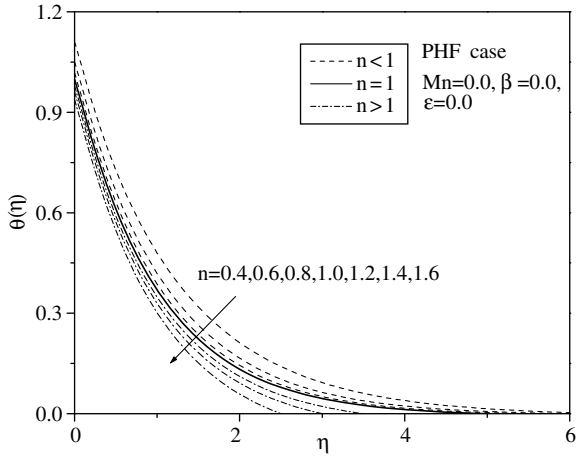

Fig. 3b. Variation of temperature profiles $\theta(\eta)$ vs. η for different values of n.

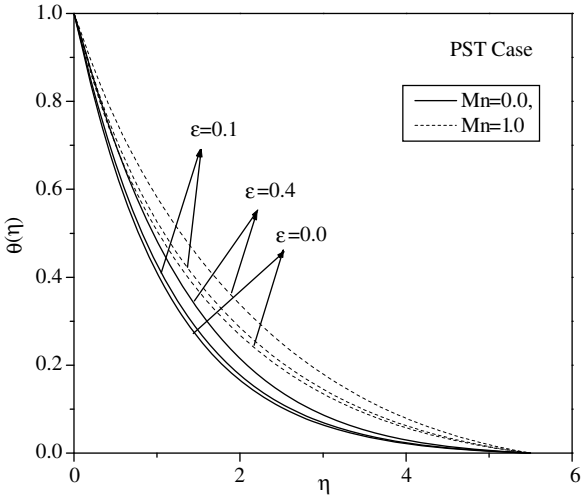

Fig. 4a. Variation of $\theta(\eta)$ vs. η for various values of Mn with $Pr = 1.0$, $\beta = 0.1$, $n = 0.8$.

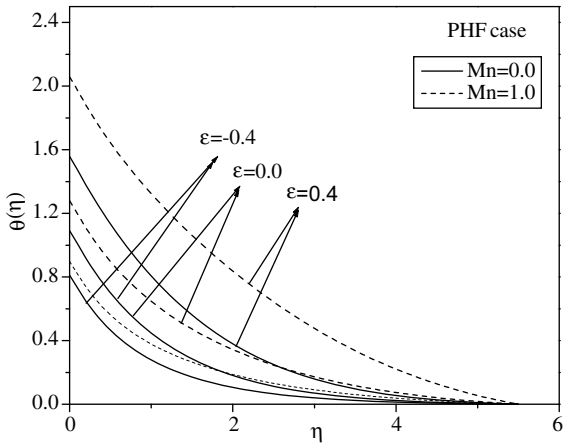

Fig. 4b. Variation of $\theta(\eta)$ vs. η for various values of Mn and ε for $n = 0.8$, $Pr = 1.0$, $\beta = 0.1$.

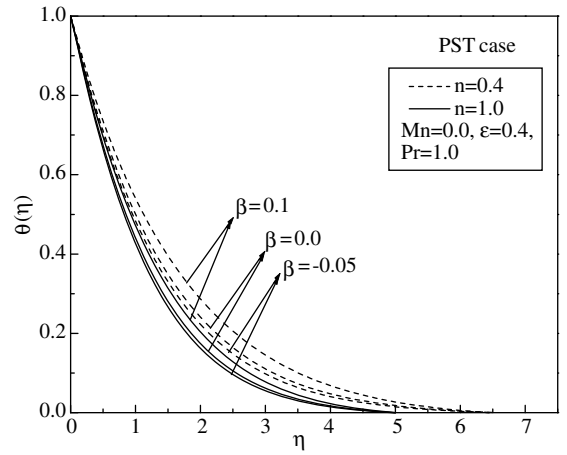

Fig. 5a. Variation of $\theta(\eta)$ vs. η for different values of β and n.

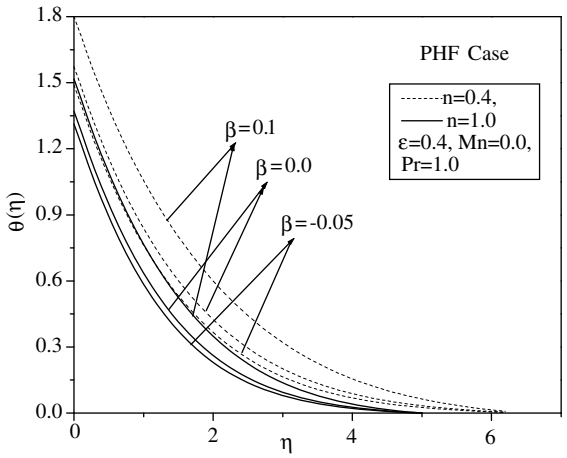

Fig. 5b. Temperature profiles $\theta(\eta)$ vs. η for different values of β and n.

The effect of power-law index, n, on temperature profiles $\theta(\eta)$ in the boundary layer for both PST and PHF cases are shown in Figs. 3a and 3b, respectively. It is observed that the temperature distribution $\theta(\eta)$ is unity at the wall in PST case and is less than the unity at the wall in PHF case for $n \geqslant 1$. However, the temperature distribution $\theta(\eta)$ for both PST and PHF cases de-

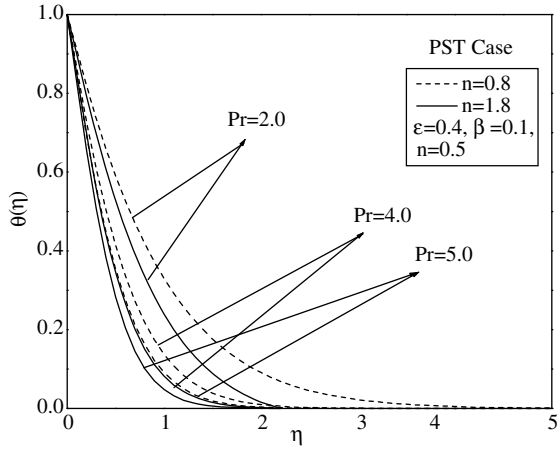

Fig. 6a. Variation of $\theta(\eta)$ vs. η for different values of Prandtl number.

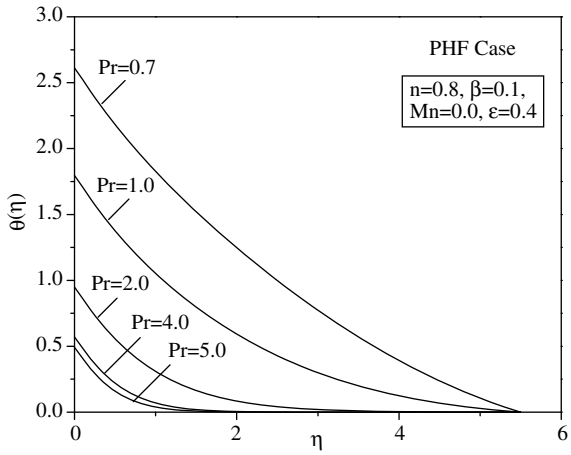

Fig. 6b. Variation of $\theta(\eta)$ vs. η for different values of Prandtl number.

Table 1
Comparison of skin friction $-f''(0)$ values with Andersson et al. [32]

	$n = 0.4$	$n = 0.6$	$n = 0.8$	$n = 1.0$	$n = 1.2$	$n = 1.5$	$n = 2.0$
Andersson et al. [32]	1.273	1.096	1.029	1.00	0.987	0.981	0.980
Present study	1.27968	1.09838	1.02897	1.00000	0.98738	0.98058	0.98035

creases asymptotically to zero in the boundary layer. The effect of increasing the values of power-law index n leads to thinning of the thermal boundary thickness. This behavior is much noticeable in shear thinning and shear thickening fluids.

The effect of magnetic parameter Mn on the temperature profile $\theta(\eta)$ in the boundary layer in presence/absence of variable thermal conductivity parameter ε for both PST and PHF cases are depicted in Figs. 4a and 4b, respectively. It is observed that the effect of magnetic field parameter Mn is to increase the temperature profile $\theta(\eta)$ and tends to zero as the space variable η increases in the boundary layer. As explained above, the introduction of a transverse magnetic field to an electrically conducting fluid gives rise to a resistive type of force known as Lorentz force. This force makes the fluid experience a resistance by increasing the friction between its layers and due to which there is increase in the temperature profile $\theta(\eta)$. This behavior is even true in the presence of non-zero values of variable thermal conductivity parameter. The effect of variable thermal conductivity parameter is to increase the temperature profile which in turn increases the thermal boundary layer thickness for both PST and PHF cases.

Figs. 5a and 5b exhibit the temperature distribution $\theta(\eta)$ with η for different values of heat source/sink parameter β in PST and PHF cases, respectively. From these graphs we observe that the temperature distribution is lower throughout the bound-

ary layer for negative values of β (heat sink) and higher for positive values of β (heat source) as compared with the temperature distribution in absence of heat source/sink parameter i.e. $\beta = 0$. Physically $\beta > 0$ implies $T_w > T_\infty$ i.e. the supply of heat to the flow region from the wall. Similarity, $\beta < 0$ implies $T_w < T_\infty$ i.e. the transfer of heat is from flow to the wall. The effect of increasing the value of heat source/sink parameter β is to increase the temperature profile $\theta(\eta)$ for both PST and PHF cases. However, minimum temperature distribution is observed in PHF case compared to PST case.

The variations of temperature profile $\theta(\eta)$ with η for various values of modified Prandtl number Pr are displayed in Figs. 6a and 6b for PST and PHF cases, respectively. Both the graphs demonstrate that the increase of Prandtl number Pr results in decrease of temperature distribution which tends to zero as the space variable η increases from the wall and hence thermal boundary layer thickness decreases as Prandtl number Pr increases for both PST and PHF cases.

The values of $-f_{\eta\eta}(0)$, which signifies the local skin friction co-efficient, C_f, are recorded in Table 2 for different values of the physical parameters n and Mn. From Table 2, we observe that $-f_{\eta\eta}(0)$ increases monotonically with increase in the magnetic field parameter Mn for various values of n. It is interesting to note that the magnitude of wall surface gradient decreases gradually with increasing power-law index for a fixed value of magnetic parameter Mn. The effect of power-law index on $-f_{\eta\eta}(0)$ is significant in shear thinning fluid ($n < 1$) then shear thickening fluid ($n > 1$). The heat transfer phenomena is usually analyzed from the numerical values of the two physical parameters i.e. (1) wall temperature gradient $-\theta_\eta(0)$ in PST case, which in turn helps in the computation of the local Nusselt number Nu_x, and (2) wall temperature $\theta(0)$ in PHF case. Numerical results for wall temperature gradient in PST case and wall temperature in PHF case are recorded in Tables 3 and 4,

Table 2
Values of skin friction $-f_{\eta\eta}(0)$ for different values of Mn and n

n	Mn = 0.0	Mn = 0.5	Mn = 1.0	Mn = 1.5	Mn = 2.0
0.4	1.292	1.8151	2.28536	2.71942	3.12702
0.6	1.107	1.4649	1.77762	2.06012	2.32088
0.8	1.034	1.3086	1.54429	1.75406	1.94588
1.0	1.0	1.2249	1.41440	1.58100	1.73200
1.2	0.989	1.1752	1.33306	1.47150	1.59599
1.4	0.982	1.1441	1.27858	1.39653	1.50229
1.6	0.980	1.1207	1.23901	1.34266	1.43425
1.8	0.979	1.1047	1.20995	1.30106	1.38230
2.0	0.978	1.0926	1.18711	1.26904	1.34174

Table 3
Wall temperature gradient $-\theta_\eta(0)$ in PST Case for $n = 0.4, 1.0, 1.8$, $\varepsilon = 0, 0.1, 0.2$ and $\beta = -0.05, 0, 0.1$

n	ε	β	Mn = 0.0					Mn = 1.0				
			$Pr = 0.7$	$Pr = 1.0$	$Pr = 2.0$	$Pr = 5.0$	$Pr = 10.0$	$Pr = 0.7$	$Pr = 1.0$	$Pr = 2.0$	$Pr = 5.0$	$Pr = 10.0$
0.4	0	−0.05	0.7539	0.934	1.4014	2.3427	3.4103	0.6329	0.7958	1.2381	2.1584	3.216
		0	0.7241	0.9005	1.3596	2.284	3.3322	0.5926	0.7492	1.1821	2.0877	3.1272
		0.1	0.6577	0.8262	1.2695	2.1606	3.1695	0.495	0.6336	1.0465	1.9324	2.938
	0.1	−0.05	0.7036	0.8722	1.3104	2.1933	3.195	0.589	0.7408	1.1544	2.0169	3.0089
		0	0.6754	0.8404	1.2708	2.1379	3.1215	0.5508	0.6964	1.1012	1.9498	2.9249
		0.1	0.6123	0.7699	1.1856	2.0214	2.9678	0.4584	0.5867	0.9716	1.8024	2.7459
	0.2	−0.05	0.661	0.8198	1.2332	2.0666	3.0125	0.5518	0.6942	1.0835	1.8968	2.833
		0	0.6339	0.7896	1.1955	2.0142	2.9428	0.5154	0.6518	1.0325	1.833	2.7533
		0.1	0.5739	0.7221	1.1143	1.9031	2.7973	0.4274	0.5465	0.9079	1.6921	2.5827
1	0	−0.05	0.8287	1.0314	1.5573	2.6001	3.7691	0.7629	0.9482	1.4586	2.5019	3.6733
		0	0.8019	1.0014	1.5208	2.5494	3.7012	0.734	0.9139	1.4159	2.4466	3.6017
		0.1	0.7439	0.9366	1.4439	2.4445	3.5616	0.6716	0.8389	1.3231	2.3307	3.4534
	0.1	−0.05	0.7727	0.9625	1.4559	2.4346	3.5317	0.7108	0.8834	1.3612	2.3403	3.4397
		0	0.7473	0.934	1.4214	2.3868	3.4679	0.6835	0.8508	1.3206	2.288	3.3722
		0.1	0.6922	0.8726	1.3481	2.2878	3.3364	0.6247	0.7797	1.2322	2.1784	3.2324
	0.2	−0.05	0.7251	0.904	1.3698	2.2944	3.3308	0.6668	0.8283	1.2784	2.2028	3.2419
		0	0.7007	0.8768	1.337	2.2487	3.2702	0.6408	0.7973	1.2396	2.1533	3.1773
		0.1	0.6482	0.8179	1.2676	2.1549	3.1453	0.5849	0.7295	1.1547	2.0491	3.0449
1.8	0	−0.05	0.9352	1.1164	1.6361	2.7354	3.968	0.914	1.0834	1.5825	2.6761	3.9121
		0	0.9164	1.0927	1.6024	2.6877	3.9045	0.8951	1.0591	1.5468	2.626	3.8466
		0.1	0.878	1.0437	1.5323	2.5893	3.7742	0.8564	1.009	1.4724	2.5221	3.7121
	0.1	−0.05	0.8758	1.044	1.5293	2.5609	3.7181	0.8563	1.013	1.4782	2.5039	3.6643
		0	0.8582	1.0214	1.4975	2.5159	3.6583	0.8387	0.9905	1.4445	2.4565	3.6026
		0.1	0.8222	0.9758	1.4312	2.4232	3.5357	0.8025	0.9438	1.3741	2.3584	3.4759
	0.2	−0.05	0.8256	0.9827	1.4387	2.4128	3.5058	0.8077	0.9538	1.3897	2.3576	3.4539
		0	0.809	0.9616	1.4084	2.3702	3.4493	0.7911	0.9323	1.3576	2.3127	3.3956
		0.1	0.7752	0.9181	1.3455	2.2822	3.3333	0.7572	0.8879	1.2907	2.2195	3.2755

Table 4
Wall temperature $\theta(0)$ in PHF case for $n = 0.4, 1.0, 1.8$, $\varepsilon = 0, 0.1, 0.2$ and $\beta = -0.05, 0, 0.1$

n	ε	β	Mn = 0.0					Mn = 1.0				
			Pr = 0.7	Pr = 1.0	Pr = 2.0	Pr = 5.0	Pr = 10.0	Pr = 0.7	Pr = 1.0	Pr = 2.0	Pr = 5.0	Pr = 10.0
0.4	0	−0.05	1.3264	1.0706	0.7136	0.4269	0.2932	1.58	1.2567	0.8077	0.4633	0.3109
		0	1.3809	1.1105	0.7355	0.4378	0.3001	1.6876	1.3348	0.846	0.479	0.3198
		0.1	1.5204	1.2104	0.7877	0.4628	0.3155	2.0203	1.5783	0.9555	0.5175	0.3404
	0.1	−0.05	1.4642	1.1582	0.751	0.4397	0.2992	1.7883	1.3852	0.8581	0.479	0.3178
		0	1.5324	1.2058	0.7756	0.4515	0.3064	1.9318	1.4836	0.9021	0.496	0.3271
		0.1	1.7108	1.3269	0.8344	0.4782	0.3225	2.4007	1.8058	1.031	0.5383	0.3488
	0.2	−0.05	1.6236	1.2564	0.7911	0.4532	0.3054	2.041	1.535	0.9134	0.4955	–
		0	1.7098	1.3136	0.8188	0.4657	0.3129	2.235	1.6605	0.9643	0.5138	0.3346
		0.1	1.9418	1.4622	0.8852	0.4945	0.3297	2.9075	2.0961	1.1184	0.5591	0.3576
1	0	−0.05	1.2067	0.9695	0.6421	0.3846	0.2653	1.3209	1.0584	0.6858	0.3997	0.2722
		0	1.247	0.9986	0.6575	0.3922	0.2702	1.3755	1.0993	0.7066	0.4087	0.2776
		0.1	1.3442	1.0677	0.6926	0.4091	0.2808	1.5114	1.2019	0.7565	0.429	0.2896
	0.1	−0.05	1.3218	1.0416	0.6724	0.3951	0.2703	1.4626	1.1476	0.7214	0.4112	0.2775
		0	1.3714	1.0758	0.6894	0.4032	0.2753	1.5311	1.1967	0.7447	0.4208	0.2831
		0.1	1.4932	1.1584	0.7285	0.421	0.2863	1.7058	1.3233	0.8013	0.4425	0.2955
	0.2	−0.05	1.4541	1.1223	0.7047	0.4059	0.2752	1.6281	1.2491	0.7598	0.4233	0.2828
		0	1.5157	1.1628	0.7236	0.4146	0.2805	1.7149	1.3092	0.7861	0.4334	0.2889
		0.1	1.6701	1.2619	0.7673	0.4334	0.292	1.9411	1.466	0.8506	0.4565	0.3016
1.8	0	−0.05	1.0693	0.8957	0.6112	0.3656	0.252	1.0772	0.9135	0.6301	0.3737	0.2556
		0	1.0912	0.9152	0.6241	0.3721	0.2561	1.0987	0.9336	0.6444	0.3808	0.26
		0.1	1.139	0.9581	0.6526	0.3862	0.265	1.1457	0.978	0.6763	0.3965	0.2694
	0.1	−-0.05	1.1523	0.9553	0.6386	0.375	0.2565	1.1598	0.9749	0.6595	0.3837	0.2602
		0	1.1778	0.9774	0.6528	0.3819	0.2607	1.1847	0.9977	0.6753	0.3912	0.2647
		0.1	1.2336	1.0267	0.6848	0.3968	0.2699	1.2391	1.0486	0.7111	0.4078	0.2745
	0.2	−0.05	1.2439	1.0198	0.6679	0.3849	0.2612	1.2502	1.0411	0.691	0.3941	0.265
		0	1.2733	1.0451	0.6835	0.3921	0.2655	1.2787	1.0672	0.7084	0.402	0.2696
		0.1	1.3373	1.1017	0.7183	0.4079	0.2749	1.3405	1.1254	0.7477	0.4196	0.2797

respectively for different non-dimensional physical parameters n, Mn, Pr, ε,β. It is observed that the effect of power-law index n is to increase the wall temperature gradient in PST case and is to decrease wall temperature in PHF case whereas reverse trend is seen with magnetic parameter Mn. This result has significant role in industrial applications to reduce expenditure on power supply in stretching the sheet just by increasing the magnetic parameter Mn. Further, it is analyzed from Table 3 that the effect of Prandtl number Pr is to decrease the wall temperature gradient in PST case and wall temperature in PHF case. In addition, the effect of increasing values of heat source/sink parameter β is to decrease the wall temperature gradient in PST case whereas its effect is to increase the wall temperature in PHF case. All the results obtained here are consistent with the physical situations.

6. Conclusions

In the present study, we have investigated MHD non-Newtonian flow over a semi-infinite non-isothermal stretching sheet with internal heat generation or absorption using Keller box method. Temperature profiles are obtained for two types of heating processes namely, PST and PHF for various values of physical parameters.

As expected, power-law index and magnetic parameters have the effect to decrease the velocity profile and reducing the boundary layer thickness. Also, increasing the value of power-law index, n, leads to thinning of thermal boundary layer thickness whereas the effect of increasing magnetic field parameter is to increase temperature profile as well as increase the thermal boundary layer thickness for both PST and PHF cases. It is noteworthy that the effect of increasing the value of heat source/sink parameter leads to increase in the temperature profile for both the PST and PHF cases. Finally, it is concluded that the thermal boundary layer thickness decreases with increase in Prandtl number for both PST and PHF cases.

Acknowledgement

One of the authors (DP) is thankful to the University Grants Commission, New Delhi for supporting financially this work under UGC-SAP (DRS-Phase-I) (Grant No. F.510/8/DRS/2004(SAP-I).

References

[1] Crane LJ. Flow past a stretching plate. Z Angew Math Phys 1970;21:645–7.
[2] Gupta PS, Gupta AS. Heat and mass transfer on a stretching sheet with suction or blowing. Can J Chem Eng 1977;55:744–6.
[3] Chen CK, Char MI. Heat transfer of a continuous stretching surface with suction or blowing. J Math Anal Appl 1988;135:568–80.

[4] Datta BK, Roy P, Gupta AS. Temperature field in the flow over a stretching sheet with uniform heat flux. Int Comm Heat Mass Transfer 1985;12:89–94.
[5] McLeod B, Rajagopal KR. On the non-uniqueness of the flow of a Navier-Stokes fluid due to stretching boundary. Arch Ration Mech Anal 1987;98:385–493.
[6] Chiam TC. Heat transfer with variable thermal conductivity in a stagnation point towards a stretching sheet. Int Comm Heat Mass Transfer 1996;23(2):239–48.
[7] Chiam TC. Heat transfer in a fluid with variable thermal conductivity over a linearly stretching sheet. Acta Mech 1998;129:63–72.
[8] Rajagopal KR, Na TY, Gupta AS. Flow of a visco-elastic fluid over a stretching sheet. Rheol Acta 1984;23:213–5.
[9] Siddappa B, Abel MS. Non-Newtonian flow past a stretching plate. Z Angew Math Phys 1985;36:47–54.
[10] Troy WC, OvermannII EA, Eremont-Rout GB, Keener JP. Uniqueness of the flow of second order fluid flow past a stretching sheet. Quart Appl Math 1987;44:753–5.
[11] Wen-Dong Chang. The non-Uniqueness of the flow of a visco-elastic fluid over a stretching sheet. Quart Appl Math 1989;47:365–6.
[12] Sam Lawrence P, Nageswara Rao B. The non-uniqueness of the MHD flow of a visco-elastic fluid past a stretching sheet. Acta Mech 1995;112:223–5.
[13] Abel MS, Veena PH. Visco-elastic fluid flow and heat transfer in a porous medium over a stretching sheet. Int J non-Linear Mech 1998;33:531–8.
[14] Bujurke NM, Biradar SN, Hiremath PS. Second order fluid flow past a stretching sheet with heat transfer. Z Angew Math Phys (ZAMP) 1987;38:653–7.
[15] Prasad KV, Subhas Abel, Khan SK. Momentum and heat transfer in a visco-elastic fluid flow in a porous medium over a non-isothermal stretching sheet. Int J Numer Meth Heat Fluid Flow 2000;10(8):786–801.
[16] Prasad KV, Subhas Abel M, Datti PS. Diffusion of chemically reactive species of a non-Newtonian fluid immersed in a porous medium over a stretching sheet. Int J Non-Linear Mech 2003;38(5):651–7.
[17] Sarpakaya T. Flow on non-Newtonian fluids in a magnetic field. Amm Inst Chem Ing J 1961;7:26–8.
[18] Pavlov KB. Magnetohydrodynamic flow of an incompressible viscous fluid caused by deformation of a plane surface. Magninaya Gidrodinamika (USSR) 1974;4:146–7.
[19] Chakrabarti A, Gupta AS. Hydromagnetic flow and heat transfer over a stretching sheet. Quart Appl Math 1979;37:73–8.
[20] Char MI. Heat and mass transfer in a hydromagnetic flow of a visco-elastic fluid over a stretching sheet. J Math Anal Appl 1994;186:674–89.
[21] Andersson HI. MHD flow of a visco-elastic fluid past a stretching surface. Acta Mech 1992;95:227–30.
[22] Datti PS, Prasad KV, Subhas Abel M, Ambuja Joshi. MHD fluid flow over a non-isothermal stretching sheet. Int J Eng Sci 2004;42:935–46.
[23] Vujannovic B, Status AM, Djukiv DJ. A variational solution of the Rayleigh problem for power law non-Newtonian conducting fluid. Ing-Arch 1972;41:381–6.
[24] Andersson HI, Bech KH, Dandapat BS. Magnetohydrodynamic flow of a power law fluid over a stretching sheet. Int J Non-Linear Mech 1992;27(6): 929–36.
[25] Jadhav JP, Waghmode BB. Heat transfer to non-Newtonian power law fluid past a continuously moving porous flat plate with heat flux. Warme und Stoffubertragung 1990;25:377–80.
[26] Savvas TA, Markatos NC, Papaspyrides CD. On the flow of non-Newtonian polymer solutions. Appl Math Model 1994;18:14–22.
[27] Cebeci T, Bradshaw P. Physical and computational aspects of convective heat transfer. New York: Springer-Verlag; 1984.
[28] Keller HB. Numerical methods for two-point boundary value problems. New York: Dover Publ.; 1992.
[29] Chiam TC. Magnetohydrodynamic heat transfer over a non-isothermal stretching sheet. Acta Mech 1997;122:169–79.
[30] Denier JP, Dabrowski PP. On the boundary layer equation for power law fluid. Proc R Soc London Ser A 2004;460:3143–58.
[31] Andersson HI, Dandapat BS. Flows of a power law fluid over a stretching sheet. Stability Appl Anal Continuous Media 1991;1:339–47.
[32] Press WH, Teukolsky SA, Vellering WT, Flannery BP. Numerical recipies in Fortran. Cambridge University Press; 1993.
[33] Conte SD, de Boor C. Elementary numerical analysis. McGraw-Hill; 1972.